First-principles equation of state and shock compression predictions of warm dense hydrocarbons

Shuai Zhang,[*,†] Kevin P. Driver,[†] and François Soubiran
Department of Earth and Planetary Science, University of California, Berkeley, California 94720, USA

Burkhard Militzer[‡]
Department of Earth and Planetary Science, University of California, Berkeley, California 94720, USA
and Department of Astronomy, University of California, Berkeley, California 94720, USA
(Received 30 January 2017; published 10 July 2017)

We use path integral Monte Carlo and density functional molecular dynamics to construct a coherent set of equations of state (EOS) for a series of hydrocarbon materials with various C:H ratios (2:1, 1:1, 2:3, 1:2, and 1:4) over the range of 0.07–22.4 g cm^{-3} and 6.7×10^3–1.29×10^8 K. The shock Hugoniot curve derived for each material displays a single compression maximum corresponding to K-shell ionization. For C:H = 1:1, the compression maximum occurs at 4.7-fold of the initial density and we show radiation effects significantly increase the shock compression ratio above 2 Gbar, surpassing relativistic effects. The single-peaked structure of the Hugoniot curves contrasts with previous work on higher-Z plasmas, which exhibit a two-peak structure corresponding to both K- and L-shell ionization. Analysis of the electronic density of states reveals that the change in Hugoniot structure is due to merging of the L-shell eigenstates in carbon, while they remain distinct for higher-Z elements. Finally, we show that the isobaric-isothermal linear mixing rule for carbon and hydrogen EOS is a reasonable approximation with errors better than 1% for stellar-core conditions.

DOI: 10.1103/PhysRevE.96.013204

I. INTRODUCTION

Hydrocarbon ablator materials are of primary importance for laser-driven shock experiments, such as those central to the study of inertial confinement fusion (ICF) [1–3] and the measurement of high energy density states relevant to giant planets [4] and stellar objects [5]. Accurate knowledge of the equation of state (EOS) of the hydrocarbon ablator is essential for optimizing experimental designs to achieve desired density and temperature states in a target. Consequently, a number of planar-driven shock wave experiments have been performed on hydrocarbon materials, including polystyrene (CH) [6–23], glow-discharge polymer (GDP) [24–28], and foams [29–32], to measure the EOS. The highest pressure achieved among these experiments is 40 Mbar [14,15], which is yet not high enough to probe the effects of K-shell ionization on the shock Hugoniot curve. Since the first x-ray scattering results on CH at above 0.1 Gbar (1 Gbar = 100 TPa) [33], ongoing, spherically converging shock experiments using the Gbar platform at the National Ignition Facility (NIF) [34–38] and the OMEGA laser [39] will extend measurements of the shock Hugoniot curve of polystyrene to pressures above 0.35 Gbar and into the K-shell ionization regime [40].

These experiments provide an important benchmark for the theoretical community working on models for EOSs of warm dense matter (WDM). EOS tables, such as SESAME [41] and QEOS [42], which are largely based on variations of Thomas-Fermi (TF) models, are outdated and yet still often used in hydrodynamic simulations for the design of shock experiments. There have been ongoing efforts to develop efficient first-principles methods for WDM that maintain an accurate treatment of the many-body and shell-ionization effects that the TF method neglects [43]. Standard Kohn-Sham density functional theory molecular dynamics (DFT-MD) is a suitable method for low and intermediate temperatures, but becomes computationally intractable beyond temperatures of 100 eV, where K-shell ionization becomes important in mid-Z elements.

The efficiency limitation of thermal DFT-MD has largely been addressed by the development of orbital-free (OF) [44] and average-atom [45] approximations. Indeed, a number of calculations employing both DFT-MD and OF-DFT have been used to study the EOS of hydrocarbon materials, including polystyrene [46–51], polyethylene [52], and GDP [26,53], in the WDM regime. The highest density and temperature simulations among these calculations have been performed with OF-DFT, up to 100 g cm^{-3} and 345 eV [50]. At low temperatures, these approximate DFT-based simulations predict the shock Hugoniot curve in good agreement with experiments. However, there are important limitations to their accuracy. OF-DFT replaces the orbital-based kinetic energy functional with a density-based TF functional and, therefore, is also unable to account for shell ionization effects [54]. On the other hand, DFT-based average atom methods only compute shell structure for an average ionic state and, subsequently, it is not well suited for studies of compounds.

As an alternative to DFT-based methods, the path integral Monte Carlo (PIMC) method [55,56] offers an approach to explicitly treat all the many-body and ionization effects as long as a suitable nodal structure is employed. Early developmental work established the accuracy of the method for fully ionized hydrogen [57,58] and helium [59] plasmas using free-particle nodes. In recent works, we have further developed free-particle [60] and localized [61] nodal structures, which has allowed us to compute first-principles EOSs across a wide range of density-temperature regimes for heavier, first- and second-row, elements.

[*]shuai.zhang01@berkeley.edu
[†]Current address: Lawrence Livermore National Laboratory, Livermore, California 94550, USA.
[‡]militzer@berkeley.edu

In this work, we combine low-temperature DFT-MD data with high-temperature PIMC data to compute coherent EOSs for several hydrocarbon materials across a wide density-temperature range. We aim to provide a highly accurate theoretical benchmark for the shock Hugoniot curves, which can help guide hydrodynamic target designs and interpret ongoing Gbar spherically converging shock experiments in the WDM regime, particulary where K-shell ionization effects arise. While such state-of-the-art shock experiments maintain exquisite control over many experimental parameters, difficulties can remain in the interpretation of results due to insufficient knowledge of the opacity in the density unfolding process of radiographic measurements [34], preheating effects, or shock uniformity and stability. Comparing both theoretical and experimental benchmarks can offer great insight into narrowing down and eliminating future sources of error.

II. METHODS

We consider five different C:H ratios of 2:1, 1:1, 2:3, 1:2, and 1:4, in order to cover the full range of interest in future shock experiments. Depending on the C:H ratio, our simulation cells contain between 30 and 50 nuclei, as well as between 100 and 130 electrons. In order to eliminate the finite-size effects at low temperatures, we use four times larger cells at temperatures up to 2×10^5 K. Above 2×10^4 K and 400 GPa, the Hugoniot curves derived with the small- and large-cell results are indistinguishable.

Using the CUPID code [62], we perform PIMC simulations within the fixed node approximation [56,63]. Similar to the PIMC simulations of hydrogen [57,58,64–70], helium [59,71], H-He mixtures [72], carbon [60,73], nitrogen [74], oxygen [75], neon [76], and water [60], we employ a free-particle nodal structure. We enforce fermion nodes at a small imaginary time interval of $1/8192$ Hartree^{-1} (Ha^{-1}) while pair density matrices [77,78] are evaluated in larger step of $1/1024$ Ha^{-1} [67].

DFT-MD simulations use the Vienna *ab initio* simulation package (VASP) [79] and exchange-correlation functionals within the local density approximation (LDA) [80,81]. We use all-electron projector augmented wave (PAW) pseudopotentials [82] with a 1.1 and a 0.8 Bohr radius core for carbon and hydrogen, respectively. We use a plane wave basis with 2000 eV cutoff, the Γ point for sampling the Brillouin zone, a MD time step of 0.05–0.2 fs, and a NVT ensemble controlled with a Nosé thermostat [83]. Typical MD trajectories consist of more than 1000 steps. Longer simulations of up to 2 ps show that the energies and pressures are converged. In order to put the DFT-MD pseudopotential energies on the same all-electron scale as PIMC calculations, we shifted all of our VASP energies by -37.4243 Ha/C and -0.445893 Ha/H. These shifts were determined by performing all-electron calculations for isolated C and H atoms with the OPIUM code [84].

III. RESULTS AND DISCUSSION

We performed DFT-MD at 6.7×10^3-10^6 K and 2–12 times the ambient density of $\rho_{\text{ambient}} = 1.05\,\text{g cm}^{-3}$. PIMC simulations were performed for 10^6–1.29×10^8 K and a much wider density range of 0.1–20 ρ_{ambient} since this method does not rely on plane-wave expansions nor pseudopotentials. At 10^6 K, the internal energy obtained from the two methods agreed to within 0.8 Ha/CH while pressures agreed to within 2%. We thus obtain a coherent first-principles EOS table [85] for hydrocarbon compounds over a wide range of temperatures and densities and show that of polystyrene (CH) in Fig. 1.

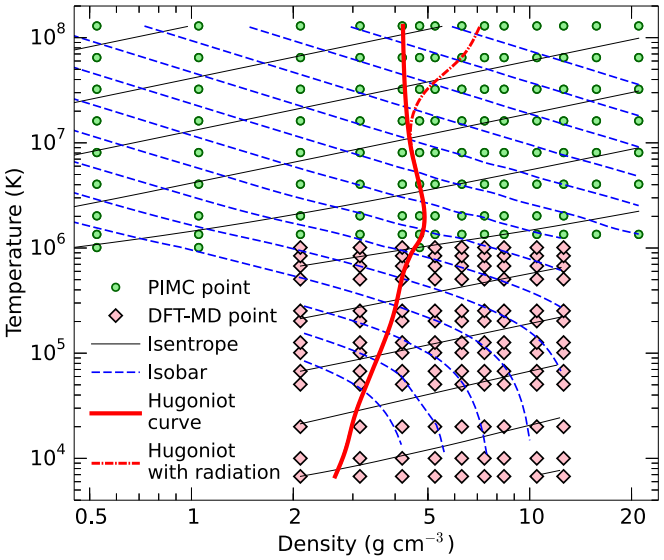

FIG. 1. Temperature-density profile of the principal Hugoniot curve of polystyrene CH (initial density $\rho_0 = 1.05\,\text{g cm}^{-3}$) with and without radiation correction, obtained from the equation of state calculated in this work. Isobar and isentrope profiles are coplotted. The symbols mark the simulation conditions.

We then use the EOS to determine the Hugoniot curves, by computing the P-V-T conditions that satisfy the Hugoniot equation $(E-E_0)+(P+P_0)(V-V_0)/2=0$, where (E_0,P_0,V_0) and (E,P,V) denote the initial and final internal energies, pressures, and volumes in a shock experiment, respectively. The initial conditions were determined based on thermophysical and thermochemical data at 1 bar [85]. For instance, the density of polystyrene at ambient is $\rho_0 = 1.05\,\text{g/cm}^3$ [86] and using the enthalpy of combustion [87] we determined $E_0 = -38.3224$ Ha/CH. The principal Hugoniot curve of polystyrene is plotted in Fig. 1. Besides the dependence of shock velocity, the shock compression is controlled by the excitation of internal degrees of freedom, which increases the compression, and interaction effects, which decrease it [71]. With increasing temperature and pressure, polystyrene is increasingly compressed until a maximum density of 4.9 g cm^{-3} reached at 2.0×10^6 K, which corresponds to the excitation of K shell electrons of carbon ions, as we will explain below.

At temperatures above 10^6 K, radiation effects can no longer be neglected. We re-construct the Hugoniot curve by considering the contribution of an ideal black-body radiation to the EOS via $P_{\text{photon}} = 4\sigma T^4/3c$ and $E_{\text{photon}} = 3P_{\text{photon}}V$, where σ is the Stefan-Boltzmann constant and c is the speed of light in vacuum. This is only an upper limit as the system is more likely to be a gray body with unknown efficiency. With the radiation contribution, the Hugoniot curve shifts to significantly higher densities at above 10^7 K and 2 Gbar, while the K-shell compression peak remains unchanged (see Fig. 1).

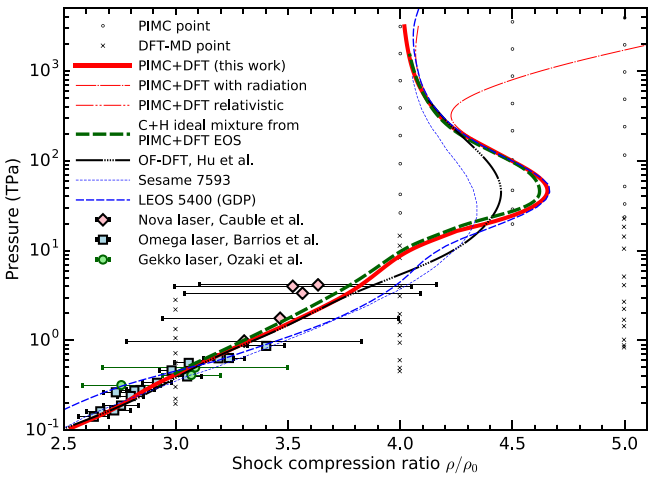

FIG. 2. Pressure-compression profile of the principal Hugoniot curve of polystyrene derived from this work in comparison with different theoretical and experimental methods: OF-DFT [50], SESAME 7593 [41], Nova [14,15], Omega [20,50] and Gekko [19] for CH, and LEOS 5400 [89] for GDP.

This shift can primarily be attributed to the photon contribution to the internal energy.

A key result of shock experiments is the relation between the compression ratio (ρ/ρ_0) and pressure. In Fig. 2, we compare our CH calculations with several experimental results and theoretical predictions. Our results are in very good agreement with experiments up to the highest pressure (4 TPa). We predict a maximum compression ratio of 4.7 at 47 TPa, which is higher than results from OF-DFT simulations (∼4.4) [50] imply and SESAME 7593 (∼4.3) [41] but similar to predictions from a semianalytical EOS model LEOS 5400 for GDP [42,88,89]. Still, all methods predict the compression maximum to occur at very similar pressures. Our DFT-MD results imply there is a small shoulder in the Hugoniot curve at 4.1-fold compression, 10^4 GPa, and 6×10^5 K, which separates in temperature the excitation regimes of the K and L shell electrons. Such a shoulder is absent from OF-DFT predictions because this method predicts the ionization to occur gradually and underestimates shell effects [54]. The shape of the SESAME Hugoniot curve is similar to that of OF-DFT, since it is largely based on TF models. The structure of the LEOS Hugoniot curve is similar to the first-principles curve, but shows significant differences at low pressures due to the existence of oxygen in GDP. Figure 2 also shows that the radiation contributions dominate over relativistic effects even though both lead to a compression ratio of 7 in the high-temperature limit, while the limit for a nonrelativistic gas is 4.

In Fig. 3, we compare our predictions for the shock Hugoniot curves of C_2H, CH, C_2H_3, CH_2, and CH_4 compounds. The initial conditions are determined by referring to representative hydrocarbon materials at ambient or cryogenic conditions [85]. For all C-H materials, we find the compression maximum to occur at very similar pressures. At the same time, we see a trend that lets the maximal compression ratio gradually decrease from 4.7 to 4.4 as the hydrogen contents is increased from C_2H to CH_4. Our Hugoniot curves of graphite and diamond

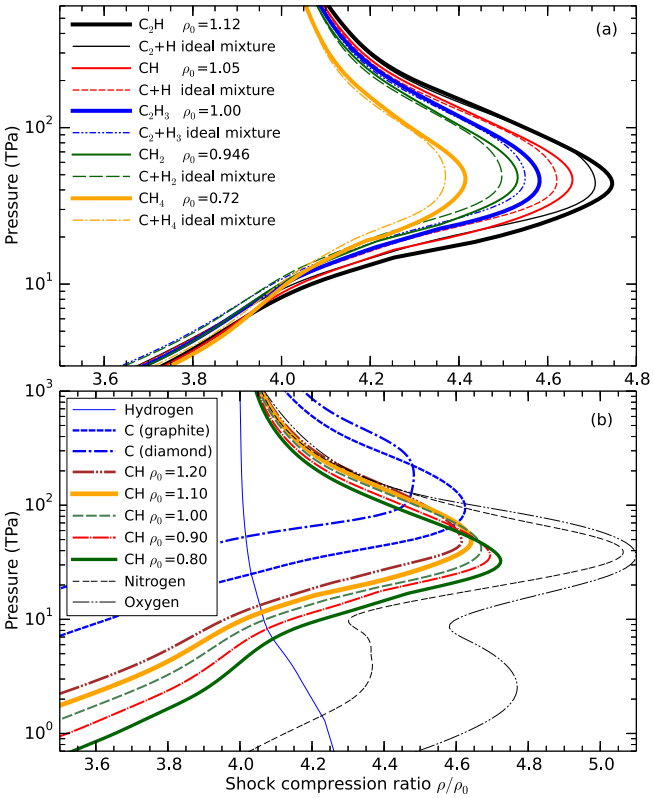

FIG. 3. (a) Hugoniot curves of C-H compounds calculated from first principles in comparison with those from ideal mixtures of carbon and hydrogen. (b) Hugoniot curves of polystyrene for different initial densities (in g cm^{-3}) and other materials.

do not follow this trend because the initial density of both materials is much higher. This implies that the particles interact more strongly under shock conditions, which reduces the shock compression ratio and shifts compression maximum towards higher pressures [71]. We also see this trend when we compare the CH Hugoniot curves for different initial densities and that of graphite and diamond with each other in Fig. 3. The compression maxima appear at a similar temperature ($\sim2\times10^6$ K) for all C-H compounds, graphite, and diamond (see Ref. [85]). This corresponds to the thermal ionization of the K shell of carbon, as we will discuss later. The magnitude of the shift in the compression maxima, ∼0.1, of the CH materials is small compared to the deviations between predictions from various EOS models in Fig. 2.

When the EOS of mixtures needs to be derived for astrophysical applications or to design shock wave experiments, one typically invokes the ideal mixing approximation because the EOS of the fully interacting systems, which we have computed here, is often not available. One simply approximates the properties of the mixture as a linear combination of the end-member properties at the same pressure and temperature. For C-H mixtures, all interactions between C and H particles are thus neglected. Furthermore, the ionization fraction of carbon atoms in the C-H mixtures is set equal to the ionization fraction of carbon at the same conditions. The presence of hydrogen does not affect the ionization of carbon atoms and vice versa.

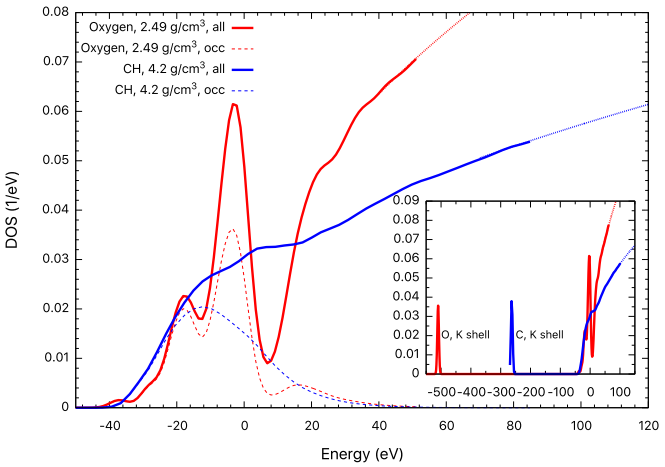

FIG. 4. Density of state of polystyrene in comparison with that of oxygen at 10^5 K. The dashed curves denote the occupied states, and the dotted lines are extrapolations of the free-electron density of state. The Fermi energies are aligned at $E = 0$ eV.

For a mixture of heavier species and metallic hydrogen at conditions in gas giant interiors, it has been shown that a linear mixing approximation was not accurate [90] while it worked very well for molecular H_2-H_2O mixtures in ice giant envelopes [91]. To test the validity of the linear mixing approximation at higher temperatures, relevant for stellar cores, we performed additional PIMC and DFT-MD simulations for pure H and C and combined them with EOS tables from Refs. [68,73]. Our results in Figs. 2 and 3 show that the linear mixing approximation works exceptionally well for all C-H compounds. We only see a small underestimation of the compression-ratio maximum of less than 1% (∼0.035). Under these conditions, the shock compression is controlled by the ionization equilibrium of K-shell electrons of the C ions. This appears to be rather insensitive to whether a C ion is surrounded by a C-H mixture or just by other C ions. We can thus anticipate that the maximum uncertainty induced by using an ideal mixing rule is below the 1% level for stellar core conditions.

Figure 3 also shows that carbon and all C-H compounds exhibit only a single compression maximum while nitrogen, oxygen, and neon [76] display two that have been attributed to the excitation of K- and L-shell electrons. The fact that carbon materials do not show the lower L-shell compression maximum of ∼3 TPa requires further investigation.

In order to better understand the difference in the Hugoniot curve shapes, we compare the electronic density of states (DOSs) in Fig. 4 that we have derived from DFT-MD simulations of oxygen and polystyrene at fourfold compression and 10^5 K. Both DOSs show an isolated peak at low energy, which corresponds to the electrons in K shells of oxygen and carbon. Their thermal ionization leads to a pronounced compression maximum along the Hugoniot curve. However, while oxygen DOS shows another set of sharp peaks corresponding to the L shell, the eigenstates of polystyrene are even distributed and partially merged with the continuum. It is the excitation of electrons in these well-defined L-shell states that leads to the second compression maximum for oxygen, nitrogen, and neon. For carbon and hydrocarbons, the L-shell ionization is much more gradual and already starts at much lower temperatures [92] than for oxygen. This does not lead to a well-defined compression peak but only to the shoulder in Hugoniot curve that we have discussed in Fig. 2.

IV. CONCLUSIONS

We performed an entirely first-principles determination of hydrocarbon mixtures in the WDM regime by including all nonideal effects. Based on PIMC and DFT-MD, we obtained coherent sets of EOS over wide range of density and temperature conditions and derived the shock Hugoniot curves of a series of hydrocarbon materials. For polystyrene, we predict a maximum shock compression ratio of 4.7 while earlier estimates range from 4.3–4.7. Our calculated Hugoniot curve agrees very well with experimental measurements and provides guidance for the interpretation of experiments on the Gbar platform at NIF. We observe a single compression maximum for hydrocarbon materials while there are two compression maxima in the Hugoniot curve of nitrogen, oxygen, and neon. We have shown that this difference is related to the properties of the L-shell ionization, which is much more gradual for carbon. We found that the linear isobaric-isothermal mixing approximation works very well, resulting in a discrepancy in the density of CH of 1% or less under stellar core conditions. This implies that it is sufficient to derive only accurate EOS tables for the end members in order to provide a thermodynamic description of deep stellar interiors.

ACKNOWLEDGMENTS

This research is supported by DOE Grants No. DE-SC0010517 and No. DE-SC0016248. F.S. and B.M. acknowledge partial support from DOE Grant DE-NA0001859. S.Z. is partially supported by the PLS-Postdoctoral Grant of the Lawrence Livermore National Laboratory. Computational support was provided by the Blue Waters sustained-petascale computing project (NSF ACI-1640776). We thank L. Benedict for helpful discussions.

[1] R. Betti and O. Hurricane, Nat. Phys. **12**, 435 (2016).
[2] N. Meezan, M. Edwards, O. Hurricane, P. Patel, D. Callahan, W. Hsing, R. Town, F. Albert, P. Amendt, L. B. Hopkins *et al.*, Plasma Phys. Controlled Fusion **59**, 014021 (2016).
[3] V. Goncharov, S. Regan, E. Campbell, T. Sangster, P. Radha, J. Myatt, D. Froula, R. Betti, T. Boehly, J. Delettrez *et al.*, Plasma Phys. Controlled Fusion **59**, 014008 (2016).
[4] T. Guillot, Annu. Rev. Earth Planet. Sci. **33**, 493 (2005).
[5] G. Wallerstein, I. Iben, P. Parker, A. M. Boesgaard, G. M. Hale, A. E. Champagne, C. A. Barnes, F. Käppeler, V. V. Smith, R. D. Hoffman *et al.*, Rev. Mod. Phys. **69**, 995 (1997).
[6] G. Hauver and A. Melani, *Shock Compression of Plexiglas and Polystyrene*, BRL Rep. No. 12591 (1964).
[7] I. Dudoladov, V. Rakitin, Y. N. Sutulov, and G. Telegin, J. Appl. Mech. Tech. Phys. **10**, 673 (1969).

[8] D. L. Lamberson, J. R. Asay, and A. H. Guenther, J. Appl. Phys. **43**, 976 (1972).

[9] S. P. Marsh, *LASL Shock Hugoniot Data* (University of California Press, Berkeley, 1980), Vol. 5.

[10] W. J. Nellis, F. H. Ree, R. J. Trainor, A. C. Mitchell, and M. B. Boslough, J. Chem. Phys. **80**, 2789 (1984).

[11] R. Kodama, K. Tanaka, M. Nakai, K. Nishihara, T. Norimatsu, T. Yamanaka, and S. Nakai, Phys. Fluids B: Plasma Phys. **3**, 735 (1991).

[12] A. V. Bushman, I. V. Lomonosov, V. E. Fortov, K. V. Khishchenko, M. V. Zhernokletov, and Yu. N. Sutulov, Zh. Eksp. Teor. Fiz. **109**, 1662 (1996) [JETP **82**, 895 (1996)].

[13] M. Koenig, A. Benuzzi, B. Faral, J. Krishnan, J. Boudenne, T. Jalinaud, C. Rémond, A. Decoster, D. Batani, D. Beretta *et al.*, Appl. Phys. Lett. **72**, 1033 (1998).

[14] R. Cauble, L. B. D. Silva, T. S. Perry, D. R. Bach, K. S. Budil, P. Celliers, G. W. Collins, A. Ng, J. T. W. Barbee, B. A. Hammel, N. C. Holmes, J. D. Kilkenny, R. J. Wallace, G. Chiu, and N. C. Woolsey, Phys. Plasmas **4**, 1857 (1997).

[15] R. Cauble, T. Perry, D. Bach, K. Budil, B. Hammel, G. Collins, D. Gold, J. Dunn, P. Celliers, L. Da Silva *et al.*, Phys. Rev. Lett. **80**, 1248 (1998).

[16] M. Koenig, F. Philippe, A. Benuzzi-Mounaix, D. Batani, M. Tomasini, E. Henry, and T. Hall, Phys. Plasmas **10**, 3026 (2003).

[17] N. Ozaki, T. Ono, K. Takamatsu, K. Tanaka, M. Nakano, T. Kataoka, M. Yoshida, K. Wakabayashi, M. Nakai, K. Nagai *et al.*, Phys. Plasmas **12**, 124503 (2005).

[18] S. Hu, V. Smalyuk, V. Goncharov, J. Knauer, P. Radha, I. Igumenshchev, J. Marozas, C. Stoeckl, B. Yaakobi, D. Shvarts *et al.*, Phys. Rev. Lett. **100**, 185003 (2008).

[19] N. Ozaki, T. Sano, M. Ikoma, K. Shigemori, T. Kimura, K. Miyanishi, T. Vinci, F. Ree, H. Azechi, T. Endo *et al.*, Phys. Plasmas **16**, 062702 (2009).

[20] M. Barrios, D. Hicks, T. Boehly, D. Fratanduono, J. Eggert, P. Celliers, G. Collins, and D. Meyerhofer, Phys. Plasmas **17**, 056307 (2010).

[21] H. Shu, S. Fu, X. Huang, G. Jia, H. Zhou, J. Wu, J. Ye, and Y. Gu, Chin. Opt. Lett. **8**, 1142 (2010).

[22] W. Shang, H. Wei, Z. Li, R. Yi, T. Zhu, T. Song, C. Huang, and J. Yang, Phys. Plasmas **20**, 102702 (2013).

[23] H. Shu, X. Huang, J. Ye, J. Wu, G. Jia, Z. Fang, Z. Xie, H. Zhou, and S. Fu, Eur. Phys. J. D **69**, 1 (2015).

[24] M. Barrios, T. Boehly, D. Hicks, D. Fratanduono, J. Eggert, G. Collins, and D. Meyerhofer, J. Appl. Phys. **111**, 093515 (2012).

[25] G. Huser, N. Ozaki, T. Sano, Y. Sakawa, K. Miyanishi, G. Salin, Y. Asaumi, M. Kita, Y. Kondo, K. Nakatsuka *et al.*, Phys. Plasmas **20**, 122703 (2013).

[26] G. Huser, V. Recoules, N. Ozaki, T. Sano, Y. Sakawa, G. Salin, B. Albertazzi, K. Miyanishi, and R. Kodama, Phys. Rev. E **92**, 063108 (2015).

[27] A. S. Moore, S. Prisbrey, K. L. Baker, P. M. Celliers, J. Fry, T. R. Dittrich, K.-J. J. Wu, M. L. Kervin, M. E. Schoff, M. Farrell *et al.*, High Energy Density Phys. **20**, 23 (2016).

[28] S. Hamel, L. X. Benedict, P. M. Celliers, M. Barrios, T. Boehly, G. Collins, T. Döppner, J. Eggert, D. Farley, D. Hicks *et al.*, Phys. Rev. B **86**, 094113 (2012).

[29] L. Bolkhovitinov and Y. B. Khvostov, Nature (London) **274**, 882 (1978).

[30] M. Koenig, A. Benuzzi, F. Philippe, D. Batani, T. Hall, N. Grandjouan, and W. Nazarov, Phys. Plasmas **6**, 3296 (1999).

[31] K. Takamatsu, N. Ozaki, K. Tanaka, T. Ono, K. Nagai, M. Nakai, T. Watari, A. Sunahara, M. Nakano, T. Kataoka *et al.*, Phys. Rev. E **67**, 056406 (2003).

[32] M. Koenig, A. Benuzzi-Mounaix, D. Batani, T. Hall, and W. Nazarov, Phys. Plasmas **12**, 012706 (2005).

[33] D. Kraus, D. A. Chapman, A. L. Kritcher, R. A. Baggott, B. Bachmann, G. W. Collins, S. H. Glenzer, J. A. Hawreliak, D. H. Kalantar, O. L. Landen, T. Ma, S. Le Pape, J. Nilsen, D. C. Swift, P. Neumayer, R. W. Falcone, D. O. Gericke, and T. Döppner, Phys. Rev. E **94**, 011202 (2016).

[34] D. C. Swift, J. A. Hawreliak, D. Braun, A. Kritcher, S. Glenzer, G. Collins, S. D. Rothman, D. Chapman, and S. Rose, AIP Conf. Proc. **1426**, 477 (2012).

[35] T. Döppner, A. Kritcher, D. Kraus, S. Glenzer, B. Bachmann, D. Chapman, G. Collins, R. Falcone, J. Hawreliak, O. Landen *et al.*, J. Phys.: Conf. Ser. **500**, 192019 (2014).

[36] A. Kritcher, T. Döppner, D. Swift, J. Hawreliak, G. Collins, J. Nilsen, B. Bachmann, E. Dewald, D. Strozzi, S. Felker *et al.*, High Energ. Dens. Phys. **10**, 27 (2014).

[37] A. Kritcher, T. Doeppner, D. Swift, J. Hawreliak, J. Nilsen, J. Hammer, B. Bachmann, G. Collins, O. Landen, C. Keane *et al.*, J. Phys.: Conf. Ser. **688**, 012055 (2016).

[38] J. Nilsen, B. Bachmann, G. Zimmerman, R. Hatarik, T. Döppner, D. Swift, J. Hawreliak, G. Collins, R. Falcone, S. Glenzer *et al.*, High Energy Density Phys. **21**, 20 (2016).

[39] R. Nora, W. Theobald, R. Betti, F. Marshall, D. Michel, W. Seka, B. Yaakobi, M. Lafon, C. Stoeckl, J. Delettrez *et al.*, Phys. Rev. Lett. **114**, 045001 (2015).

[40] T. Doeppner and A. Kritcher (private communication).

[41] *SESAME: The Los Alamos National Laboratory Equation of State Database*, edited by S. P. Lyon and J. D. Johnson (Group T-1, Report No. LA-UR-92-3407, 1992).

[42] R. More, K. Warren, D. Young, and G. Zimmerman, Phys. Fluids **31**, 3059 (1988).

[43] *Frontiers and Challenges in Warm Dense Matter*, edited by F. Graziani, M. P. Desjarlais, R. Redmer, and S. B. Trickey (Springer, Berlin, 2014).

[44] F. Lambert, J. Clérouin, and G. Zérah, Phys. Rev. E **73**, 016403 (2006).

[45] B. Wilson, V. Sonnad, P. Sterne, and W. Isaacs, J. Quantum Spectrosc. Radiat. Transfer **99**, 658 (2006).

[46] T. R. Mattsson, J. M. D. Lane, K. R. Cochrane, M. P. Desjarlais, A. P. Thompson, F. Pierce, and G. S. Grest, Phys. Rev. B **81**, 054103 (2010).

[47] C. Wang, X.-T. He, and P. Zhang, Phys. Plasmas **18**, 082707 (2011).

[48] F. Lambert and V. Recoules, Phys. Rev. E **86**, 026405 (2012).

[49] S. X. Hu, T. R. Boehly, and L. A. Collins, Phys. Rev. E **89**, 063104 (2014).

[50] S. X. Hu, L. A. Collins, V. N. Goncharov, J. D. Kress, R. L. McCrory, and S. Skupsky, Phys. Rev. E **92**, 043104 (2015).

[51] S. X. Hu, L. A. Collins, V. N. Goncharov, J. D. Kress, R. L. McCrory, and S. Skupsky, Phys. Plasmas **23**, 042704 (2016).

[52] D. Knyazev and P. Levashov, Phys. Plasmas **22**, 053303 (2015).

[53] P. Colin-Lalu, V. Recoules, G. Salin, T. Plisson, E. Brambrink, T. Vinci, R. Bolis, and G. Huser, Phys. Rev. E **94**, 023204 (2016).

[54] S. X. Hu, B. Militzer, L. A. Collins, K. P. Driver, and J. D. Kress, Phys. Rev. B **94**, 094109 (2016).

[55] D. M. Ceperley, Rev. Mod. Phys. **67**, 279 (1995).
[56] D. M. Ceperley, in *Monte Carlo and Molecular Dynamics of Condensed Matter Systems*, edited by K. Binder and G. Ciccotti (Editrice Compositori, Bologna, 1996), Vol. 49, p. 443.
[57] C. Pierleoni, D. M. Ceperley, B. Bernu, and W. R. Magro, Phys. Rev. Lett. **73**, 2145 (1994).
[58] B. Militzer and D. M. Ceperley, Phys. Rev. E **63**, 066404 (2001).
[59] B. Militzer, Phys. Rev. B **79**, 155105 (2009).
[60] K. P. Driver and B. Militzer, Phys. Rev. Lett. **108**, 115502 (2012).
[61] B. Militzer and K. P. Driver, Phys. Rev. Lett. **115**, 176403 (2015).
[62] B. Militzer, Ph.D. thesis, University of Illinois at Urbana-Champaign, 2000.
[63] D. M. Ceperley, J. Stat. Phys. **63**, 1237 (1991).
[64] W. R. Magro, D. M. Ceperley, C. Pierleoni, and B. Bernu, Phys. Rev. Lett. **76**, 1240 (1996).
[65] B. Militzer, D. M. Ceperley, J. D. Kress, J. D. Johnson, L. A. Collins, and S. Mazevet, Phys. Rev. Lett. **87**, 275502 (2001).
[66] S. X. Hu, B. Militzer, V. N. Goncharov, and S. Skupsky, Phys. Rev. Lett. **104**, 235003 (2010).
[67] B. Militzer and D. M. Ceperley, Phys. Rev. Lett. **85**, 1890 (2000).
[68] S. X. Hu, B. Militzer, V. N. Goncharov, and S. Skupsky, Phys. Rev. B **84**, 224109 (2011).
[69] B. Militzer, W. Magro, and D. Ceperley, Contrib. Plasma Phys. **39**, 151 (1999).
[70] B. Militzer and R. L. Graham, J. Phys. Chem. Solids **67**, 2136 (2006).
[71] B. Militzer, Phys. Rev. Lett. **97**, 175501 (2006).
[72] B. Militzer, J. Low Temp. Phys. **139**, 739 (2005).
[73] L. X. Benedict, K. P. Driver, S. Hamel, B. Militzer, T. Qi, A. A. Correa, A. Saul, and E. Schwegler, Phys. Rev. B **89**, 224109 (2014).
[74] K. P. Driver and B. Militzer, Phys. Rev. B **93**, 064101 (2016).
[75] K. P. Driver, F. Soubiran, S. Zhang, and B. Militzer, J. Chem. Phys. **143**, 164507 (2015).
[76] K. P. Driver and B. Militzer, Phys. Rev. B **91**, 045103 (2015).
[77] E. L. Pollock, Comput. Phys. Commun. **52**, 49 (1988).
[78] B. Militzer, Comput. Phys. Commun. **204**, 88 (2016).
[79] G. Kresse and J. Furthmüller, Phys. Rev. B **54**, 11169 (1996).
[80] J. P. Perdew and A. Zunger, Phys. Rev. B **23**, 5048 (1981).
[81] D. M. Ceperley and B. J. Alder, Phys. Rev. Lett. **45**, 566 (1980).
[82] P. E. Blöchl, O. Jepsen, and O. K. Andersen, Phys. Rev. B **49**, 16223 (1994).
[83] S. Nosé, J. Chem. Phys. **81**, 511 (1984).
[84] http://opium.sourceforge.net.
[85] See Supplemental Material at http://link.aps.org/supplemental/10.1103/PhysRevE.96.013204 for the way of determining the initial conditions for the shock Hugoniot curves, shock Hugoniot curves in temperature-compression ratio plots, the nuclear pair correlation function at different densities and temperatures, and details of the EOS data.
[86] NIST/TRC Web Thermo Tables (WTT) NIST Standard Reference Subscription Database 3 - Professional Edition Version 2-2012-1-Pro, http://wtt-pro.nist.gov/wtt-pro/.
[87] R. N. Walters, S. M. Hackett, and R. E. Lyon, Fire Mater. **24**, 245 (2000).
[88] D. A. Young and E. M. Corey, J. Appl. Phys. **78**, 3748 (1995).
[89] P. A. Sterne, L. X. Benedict, S. Hamel, A. A. Correa, J. L. Milovich, M. M. Marinak, P. M. Celliers, and D. E. Fratanduono, J. Phys.: Conf. Ser. **717**, 012082 (2016).
[90] F. Soubiran and B. Militzer, Astrophys. J. **829**, 14 (2016).
[91] F. Soubiran and B. Militzer, Astrophys. J. **806**, 228 (2015).
[92] A. Y. Potekhin, G. Massacrier, and G. Chabrier, Phys. Rev. E **72**, 046402 (2005).